Synthesis and electronic properties of nitrogen-bridged dimers of boron subphthalocyanines

Received 00th January 20xx,
Accepted 00th January 20xx

DOI: 10.1039/x0xx00000x

www.rsc.org/

J. Guilleme,[a,b] D. Gonzalez-Rodriguez[b]* and T. Torres[a,b]*

The synthesis of new symmetric and unsymmetric axial nitrogen-bridged dimers of subphthalocyanines (μ-azo dimers) has been carried out via activated triflate intermediates. Their spectroscopic and electrochemical properties have been studied and compared to their μ-oxo analogues.

Subphthalocyanines (SubPcs),[1] the lower relatives of Phthalocyanines (Pcs),[2] are unique non-planar aromatic macrocycles whose structure comprises three units of diiminoisoindole arranged in a cone-shaped structure around a central boron atom. During the last two decades, these compounds have emerged as potential candidates in several applied fields due to their appealing photophysical features and their tunable electronic properties.[3]

Expanding the π-surface of SubPcs results in new varieties of subazamacrocycles with intriguing electronic features. For instance, SubPc dimers[4] can be generated by condensation of two molecules through either the axial position, leading to μ-oxo dimers linked together by a single oxygen atom,[5] or through the peripheral positions, leading to the so-called "fused dimers" where two isoindole units share a common benzene ring (Figure 1).[6] These dimeric species usually display a dramatic change in their optoelectronic properties as a consequence of their π-overlapped or π-extended systems, respectively. For instance, μ-oxo dimers exhibit blue-shifted, broadened absorption *Q*-bands in comparison to monomeric SubPcs,[5] whereas fused SubPc systems expand their absorption spectra toward the red region.[6]

First reported in 1996 by Geller *et al.*, μ-oxo dimers have been mostly described as a common byproduct in the axial ligand exchange reaction of SubPcs. Recently, two different attempts to obtain μ-oxo dimers as major products have been carried out, leading to their formation in moderate yields (*ca.* 30 %).[5c,d] Furthermore, μ-oxo dimers have been made unsymmetric, that is, with one SubPc moiety different from the other. The development of these synthetic routes may open the door to the design of donor-acceptor complexes in which both moieties are close enough to interact with each other ensuing the overlapping of their molecular orbitals, and thus enabling interesting electron and energy transfer phenomena.[7]

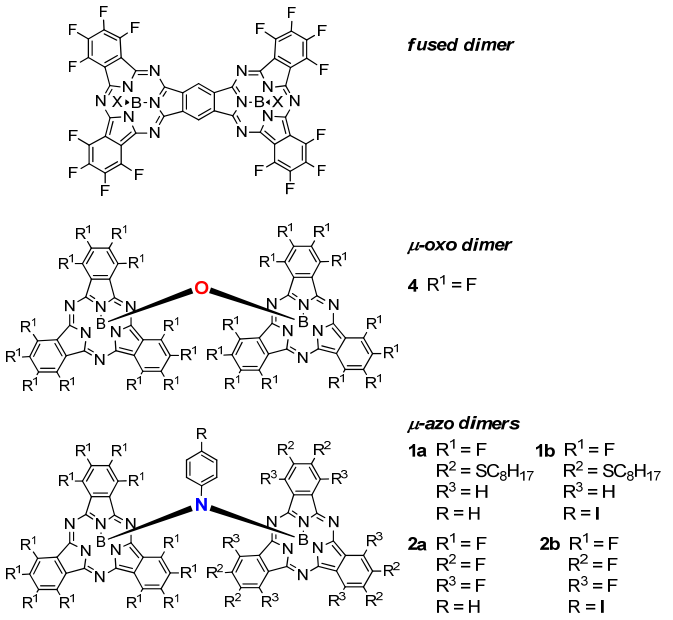

Figure 1. Chemical structure of fused π-extended, μ-oxo (**4**), and the novel μ-azo (**1a-b**, **2a-b**) SubPc dimers prepared and studied in this work.

Despite the importance of these axially-linked molecular systems, no examples of nitrogen-bridged SubPc dimers have been reported hitherto. In addition to the challenge that the synthesis of these molecules represent, we were very intrigued by how the nitrogen bridge would affect the electronic properties of the ensemble. Both distance and angles between SubPcs would be influenced by the nature of the bridging atom, and this should tune orbital overlap and hence spectroscopic and redox features. Besides, the nitrogen

[a] *IMDEA Nanociencia, Faraday 9, Campus Cantoblanco, 28049, Spain.*
[b] *Departamento Química Orgánica, Facultad de Ciencias, Universidad Autónoma de Madrid, E-28049 Madrid, Spain*
Email: tomas.torres@uam.es; david.gonzalez.rodriguez@uam.es
Electronic Supplementary Information (ESI) available: [details of any supplementary information available should be included here]. See DOI: 10.1039/x0xx00000x

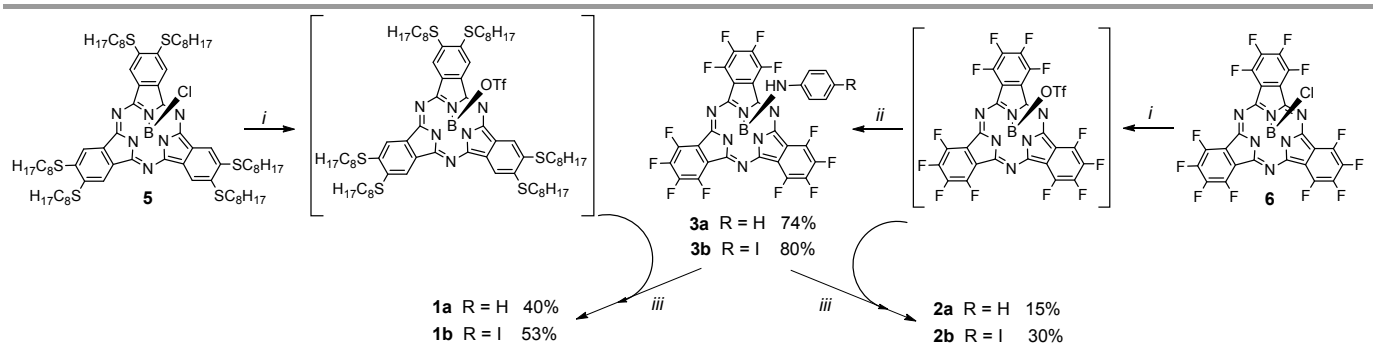

Scheme 1. Synthetic route to obtain **1a**-**b**, **2a**-**b** and **3a**-**b**. i) Toluene, AgOTf; ii) Aniline or 4-iodoaniline, DiPEA, rt; iii) Toluene, DiPEA, reflux.

bridge, bearing an additional functionalizable position, may be used for the construction of more complex systems. Here, we report on the stepwise synthesis and characterization of symmetric and unsymmetric μ-azo SubPc dimers.

The synthetic route toward μ-azo dimers **1** and **2** (Scheme 1) involves a common step which relies on the isolation of monomeric SubPc **3**, which will be employed as a nucleophile in the subsequent axial substitutions.[8] In order to obtain **3**, (dodecafluoro)SubPcBCl was subjected to an axial ligand exchange reaction through the intermediacy of an activated triflate intermediate,[9] employing aniline or 4-iodoaniline as nucleophiles to afford, respectively, SubPcs **3a** and **3b**. Then, SubPc **3a**/**b** was added to the corresponding activated triflate from hexa(octylthio)SubPcBCl or (dodecafluoro)SubPcBCl, and heated to reflux in toluene to obtain the desired μ-azo dimers **1a-b** and **2a-b** in moderate yields. The introduction of reactive functionalities at the nitrogen bridge, such as the iodoarene in the **b** series, opens the door to the incorporation of these μ-azo SubPc compounds in systems of higher complexity where, for instance, a third photoactive unit could be coupled. All the new compounds were characterized by ^{1}H, ^{19}F (see Figure S1) and ^{13}C NMR, MS, HR-MS and UV-vis.

The effect of the aromatic ring current of the SubPc macrocycle(s) in the chemical shift of the axial aniline protons can be compared in the ^{1}H NMR spectrum of **3** and **2** (Figure 2). The *ortho*- and, to a lower extent, *meta*-protons (***o*-** and ***m*-**, respectively, in Figure 2) of the aniline moiety experience an increasing upfield shift as this axial ligand is substituted with one (**3**) or two (**2**) SubPc macrocycles.

UV-vis absorption and emission spectra of **1**, **2, 3** and ((dodecafluoro)SubPcB)$_2$O μ-oxo dimer (**4**) were registered in different solvents at room temperature (Figure 3) to evaluate any solvent polarity effects. Both the non-iodinated (**a**) and iodinated (**b**) series display the same behavior, so from now on we will only comment on the properties of the former. As

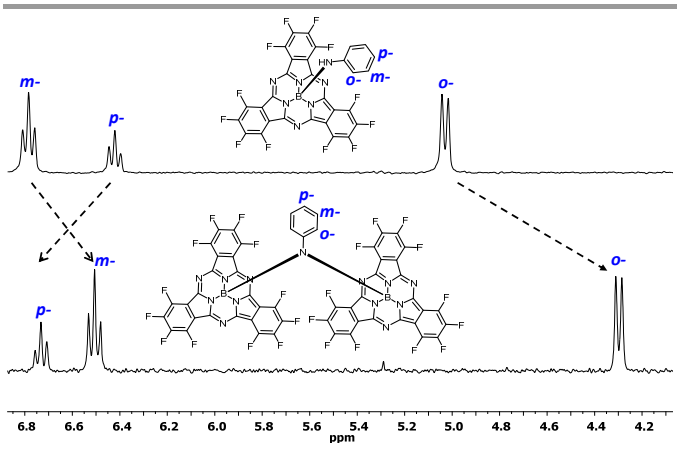

Figure 2. Region of the ^{1}H NMR of **3a** and **2a** ($CDCl_3$). The arrows indicate the shifts experienced by the axial aniline *ortho*-, *meta*- and *para*- protons.

shown in Figure 3a, SubPc **3a** displays the typical *Q*-band characteristic of monomeric species with λ_{max} (**3a**) = 570 nm. On the contrary, the *Q*-band maxima of μ-azo dimers **1a** and **2a** (Table 1) exhibit blue shifts (λ_{max} (**1a**) = 560 nm; λ_{max} (**2a**) = 548 nm), and a significant broadening, with blue- and red-shifted shoulders at λ = 518, 598 and *ca.* 680 nm for **1a** and λ = 511, 576 and 625 nm for **2a**. This perturbation of the SubPc electronic transitions has been previously ascribed in μ-oxo dimers to isoindole π-π overlap between the two adjacent macrocycles.[5c,d] The blue absorption shift suffered by these μ-azo dimers is slightly smaller than the one observed for μ-oxo dimer **4** (λ_{max} (**4**) = 543 nm), but the *Q*-band structure is very similar. Compound **1a** also displays characteristic absorption bands around 400 nm, attributed to n→π* transitions in the thioether-substituted SubPc. The absorption spectra of the four compounds remain almost unaltered when changing solvent from toluene to benzonitrile (see Figure S2), so charge-transfer interactions are unlikely.

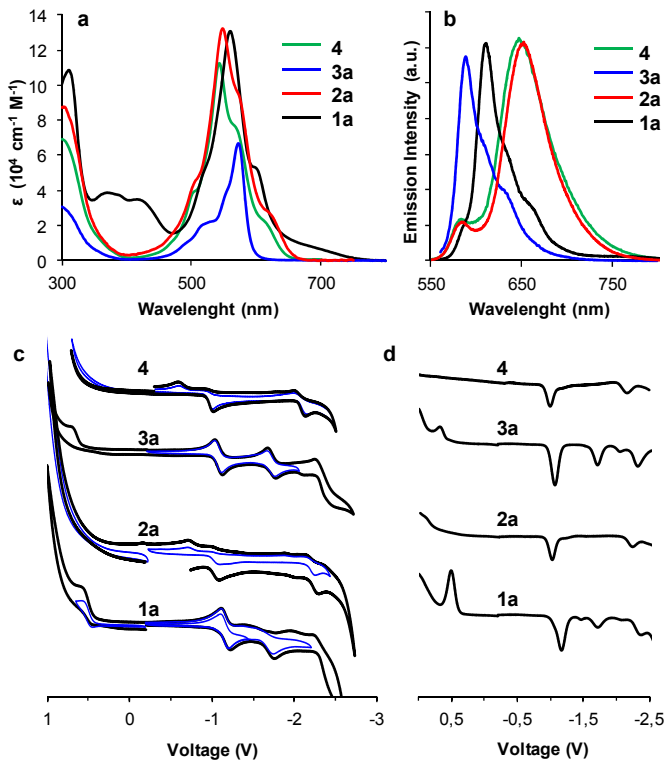

Figure 3. **a**) UV-vis and **b**) normalized emission spectra (λ_{exc} = 530 nm) of **1a** (black), **2a** (red), **3a** (blue) and **4** (green) in toluene. **c**) Cyclic voltammograms (CVs) and **d**) Osteryoung Square Wave voltammograms (OSWVs) for compounds **1a**, **2a**, **3a** and **4** in degassed THF-TBAPF$_6$ solutions relative to Fc/Fc$^+$ at r.t.

Steady state fluorescence experiments were also carried out in toluene at room temperature for **1**-**4** (Figure 3b and Table 1). All compounds display a single maximum that is strongly red shifted in the case of the dimers (λ_{max} (**1a**) = 610 nm, λ_{max} (**2a**) = 652 nm, λ_{max} (**4**) = 644 nm) in comparison with monomer species (λ_{max} (**3a**) = 588 nm). This data underlines the sensibility of the fluorescence emission features to peripheral SubPc substitution, as was also noted in other unsymmetrical axially connected species.[5d,e] Together with the absorption data, this information reveals Stokes shifts considerably larger than those of monomeric SubPcs: 50 nm for the unsymmetric μ-azo dimer (**1a**), 104 nm for the symmetric one (**2a**), and 101 nm for the symmetric μ-oxo dimer **4** (Table 1).

Fluorescence quantum yields (ϕ_F) were measured in toluene employing (triiodo)SubPcBOPh (ϕ_F = 0.08) as external reference.[10] Remarkably low values were calculated for **1a**, **2a**, **3a** and **4** revealing the non-emissive nature of these products. As stated before, the structure of these *H*-type dimers, in which two SubPcs are close enough to π-π interact with each other, may lead to self-quenching phenomena in diluted solutions. On the other hand, monomeric SubPc (**3**) present a similar ϕ_F, leading to conclude that the aniline moiety also plays a role in the fluorescence deactivation pathways. This emission quenching has been previously observed in a related (dodecafluoro)SubPc with an axial phenothiazine group, and was ascribed to fast intramolecular electron transfer events.[11]

Next, the electrochemical properties of the new μ-azo derivatives were evaluated by cyclic voltammetry in THF solutions (Figure 3c,d). We were particularly interested in evaluating the influence of the second SubPc moiety, having an electron-rich (**1**) or electron-poor (**2** and **4**) character, on the redox processes of the common (dodecafluoro)SubPc macrocycle when comparing dimers and monomer. The redox data, collected in Table 1, indicates that the first reduction event becomes more negative in the order **2a** ~ **4** < **3a** < **1a**, indicating that the second SubPc moiety facilitates reduction if it is electron-poor and makes it more difficult when it is electron-rich. A closer look into the voltammograms also reveals that **2a** and **4** follow very similar reduction behavior: the first reduction processes of the (dodecafluoro)SubPc moieties being intimately related and occurring just below and above -1 V, while the second reduction of this macrocycle occurs at more negative potentials than in **3a**, due to the influence of the adjacent negatively charged SubPc. On the contrary, **1a** displays cathodic waves that resemble the behavior of **3a**, and the reduction of each SubPc unit takes place at separated potentials. In the anodic part of the voltammograms, the oxidation of the hexa(octylthio)SubPc moiety in **1a** was detected at +0.51 V, which is in agreement with previously measured data of SubPcs with this peripheral substitution.[12] Axial aniline oxidation could only be clearly observed for **3a** at +0.67 V.

Table 1. Photophysical and redox data measured for compounds **1a**, **2a**, **3a** and **4**.

	λ_{max}^{abs} (nm)[a]	λ_{max}^{em} (nm)[a]	ϕ_{PL}[a,b]	E^1_{ox} (V)[c]	E^1_{red} (V)[c]
1a	560	610	0.03	+0.51	-1.16
2a	548	652	0.02	-	-1.02 (2e)
3a	570	588	0.04	+0.67	-1.07
4	543	644	0.05	-	-0.98 (2e)

[a] In toluene solution. [b] Relative to a I$_3$SubPcBOPh standard (ϕ_F = 0.08). [c] OSWV peak potentials measured in THF-TBAPF$_6$ solutions relative to Fc/Fc$^+$ at r.t.

In order to shed light into the electronic characteristics of this novel family of compounds, DFT calculations (B3LYP/6-31G(d,p)) were performed on model structures of **1a** (octyl chains replaced by methyl), **2a**, **3a** and **4**. The most relevant frontier orbitals (HOMO–1 → LUMO+1) and their energies are plotted in Figure 4. The optimized structures of μ-azo dimers **1a** and **2a** display B-N distances of 1.53 Å and B-N-B bond angles of 130°. On the contrary, a shorter B-O distance of 1.38 Å and a wider B-O-B angle of 137° were determined for the μ-oxo analogue **4**. Hence, π-orbital overlap is extended in the μ-azo dimers, since the interacting isoindole units are arranged in parallel. Although the absolute energy DFT values are lower than expected, calculations predict a considerable stabilization of the LUMO orbital for dimers **2a** and **4**, which is consistent with the lower first reduction potential observed in the forward cathodic scans, when compared to monomer **3a**. The presence of the donor thioether-substituted ring in **1a** results in a significant stabilization of the HOMO orbital, localized on this moiety, and hence in a lower HOMO-LUMO gap.

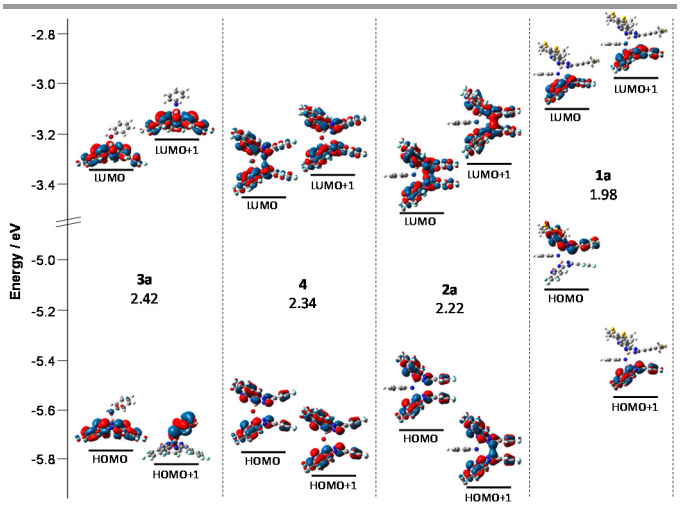

Figure 4. DFT-calculated (B3LYP/6-31G(d,p)) frontier orbitals (HOMO–1 → LUMO+1) of model structures of **1a** (octyl chains replaced by methyl), **2a**, **3a** and **4**. HOMO-LUMO gap energies (in eV) are indicated for each compound.

In conclusion, a new family of μ-azo dimers has been synthesized by means of consecutive axial ligand substitutions through the intermediacy of activated electrophilic triflate-SubPcs. The spectroscopic and electrochemical properties of the new compounds have been analyzed and compared to their closer μ-oxo dimer analogues. Even though the optimized molecular geometries are somewhat different, the effect of the bridging atom (i.e. N *versus* O) does not seem to influence significantly the electronic properties of these double bell-shaped π-conjugated molecules. However, as it occurs with π-oxo dimers,[5d] the combination of SubPc macrocycles with different electronic character[13] brings about marked alterations of the electronic levels. Finally, one of the main advantages of introducing amine functions into these μ-bridged dimers is that they leave the door open for further functionalization.

Acknowledgements

Financial support from the MINECO, Spain (CTQ-2014-52869-P, T.T.; CTQ2014-57729-P, D.G.-R.), the Comunidad de Madrid (S2013/MIT-2841 FOTOCARBON, T.T.) and the European Research Council (ERC-StG 279548, D.G.-R.) is acknowledged. The work of J.G. was funded by MECD (FPU fellowship).

Notes and References

1 (a) C. G. Claessens, D. González-Rodríguez, T. Torres, *Chem. Rev.*, 2002, **102**, 835-853; (b) T. Torres, *Angew. Chem. Int. Ed.*, 2006, **45**, 2834-2837; (c) P. J. Brothers, *Chem. Commun*., 2008, 2090–2102; (d) S. Shimizu, N. Kobayashi, *Chem. Commun.,* 2014, **50,** 6949-6966; (e) C. G. Claessens, D. González-Rodríguez, M. S. Rodríguez-Morgade, A. Medina, T. Torres, *Chem. Rev.*, 2014, **114**, 2192-2277.

2 (a) G. de la Torre, C. G. Claessens, T. Torres, *Chem. Commun.*, 2007, 2000; (b) C. G. Claessens, U. Hahn, T. Torres, *Chem. Rec.*, 2008, **8**, 75-97; (c) J. Mack, N. Kobayashi, *Chem. Rev*., 2011, **111**, 281-321. (d) G. Bottari, G. de la Torre, T. Torres, *Acc. Chem. Res.*, 2015, **48**, 900–910.

3 (a) G. E. Morse, T. P Bender, *ACS Appl. Mater. Interfaces*, 2012, **4**, 5055-5068; (b) K. Cnops, B. P. Rand, D. Cheyns, B. Verreet, M. A. Empl, P. Heremans, *Nat. Commun.*, 2014, **5**, 3406; (c) K. Cnops, G. Zango, J. Genoe, P. Heremans, M. V. Martinez-Diaz, T. Torres, D. Cheyns, *J. Am. Chem. Soc.*, 2015, **137**, 8991−8997; (d) Y. Zou, R. J. Holmes, *ACS Appl. Mater. Interfaces*, 2015, **7**, 18306−18311; (e) J. Endres, I. Pelczer, B. P. Rand, A. Kahn, *Chem. Mater*., 2016, **28**, 794-801.

4 N. Kobayashi, *Coord. Chem. Rev.*, 2002, **227**, 129-152.

5 (a) M. Geyer, F. Plenzig, J. Rauschnabel, M. Hanack, B. del Rey, A. Sastre, T. Torres, *Synthesis*, 1996, 1139–1151; (b) N. Kobayashi, *J. Porphyrins Phthalocyanines,* 1999, **3**, 453-467; (c) Y. Yamasaki, T. Mori, *Bull. Chem. Soc. Jpn.,* 2011, **84**, 1208-1214; (d) J. D. Dang, M. V. Fulford, B. A. Kamino, A. S. Paton, T. P. Bender, *Dalton Trans.*, 2015, **44**, 4280–4288; (e) S. Mori, N. Ogawa, E. Tokunaga, N. Shibata, *Dalton Trans.* 2015, **44**, 19451–19455.

6 (a) N. Kobayashi, *J. Chem. Soc., Chem. Commun*., 1991, 1203-1205; (b) C. G. Claessens, T. Torres, *Angew. Chem. Int. Ed.*, 2002, **41**, 2561-2565; (c) T. Fukuda, J. R. Stork, R. J. Potucek, M. M. Olmstead, B. C. Noll, N. Kobayashi, W. S. Durfee, *Angew. Chem. Int. Ed.*, 2002, **41**, 2565-2568; (d) R. S. Iglesias, C. G. Claessens, T. Torres, G. M. A. Rahman, D. M. Guldi, *Chem. Commun.*, 2005, 2113-2115; (c) G. Zango, J. Zirzlmeier, C. G. Claessens, T. Clark, M. V. Martínez-Díaz, D. M. Guldi, T. Torres, *Chem. Sci.*, 2015, **6**, 5571-5577.

7 (a) C. G. Claessens, D. González-Rodríguez, R. S. Iglesias, T. Torres, *C. R. Chimie*, 2006, **9**, 1094-1099; (b) D. González-Rodríguez, G. Bottari, *J. Porphyrins Phthalocyanines*, 2009, **13**, 624-636; (c) C. Romero Nieto, J. Guilleme, C. Villegas, J. L. Delgado, D. González-Rodríguez, N. Martín, T. Torres, D. M. Guldi, *J. Mater. Chem.*, 2011, **21**, 15914-15918; (d) V. Bandi, F. P. D'Souza, H. B. Gobeze, F. D'Souza, *Chem. Commun.,* 2016, **52**, 579-581.

8 J. Guilleme, L. Martínez-Fernández, D. González-Rodríguez, I. Corral, M. Yáñez, T. Torres, *J. Am. Chem. Soc.*, 2014, **136**, 14289-14298.

9 (a) J. Guilleme, D. González-Rodríguez, T. Torres, *Angew. Chem. Int. Ed.*, 2011, **50**, 3506–3509; (b) J. Guilleme, L. Martínez-Fernández, I. Corral, M. Yáñez, D. González-Rodríguez, T. Torres, *Org. Lett.*, 2015, **17**, 4722–4725.

10 D. González-Rodríguez, T. Torres, D. M. Guldi, J. Rivera, M. A. Herranz, L. Echegoyen, *J. Am. Chem. Soc.*, 2004, **126**, 6301-6313.

11 a) C. Romero-Nieto, J. Guilleme, J. Fernández-Ariza, M. S. Rodríguez-Morgade, D. González-Rodríguez, T. Torres, D. M. Guldi, *Org. Lett.*, 2012, **14**, 5656-5659; b) Y. Bernhard, P. Winckler, R. Chassagnon, P. Richard, E. Gigot, J.-M. Perrier-Cornet, R. A. Decreau, *Chem. Commun.* 2014, **50**, 13975-13978.

12 (a) R. S. Iglesias, C. G. Claessens, T. Torres, M. A. Herranz, V. A. Ferro, J. M. García de la Vega, *J. Org. Chem.*, 2007, **72**, 2967-2977; (b) D. González-Rodríguez, M. A. Martínez-Díaz, J. Abel, A. Perl, J. Huskens, L. Echegoyen, T. Torres, *Org. Lett.*, 2010, **12**, 2970-2973.

13 S. Mori, N. Ogawa, E. Tokunaga, S. Tsuzukic, N. Shibata, *Dalton Trans.*, 2016, **45**, 908-912.